AADE-23-NTCE-065

Digital Rock Lab Enables Application-Specific Three-Dimensional Cutter Development and Its Application in Haynesville Shale Lateral Drilling

Xiaoge Gan, Curtis Byrd, Yuri Burhan, Wiley Long, Youhe Zhang, SLB

Abstract

In recent years there's been rapid growth of three-dimensional cutter (3DC) usage in various drilling applications all over the world. Testing in both field and laboratory environments have shown that 3DC is more advantageous than the conventional flat-top polycrystalline diamond compact (PDC) cutter for cutting efficiency and formation adaptability. Because of advanced laser-etching technology, nowadays almost any shaped cutter can be produced and deployed in the field in a matter of weeks or even days. However, challenges remain on how a 3DC can be developed to meet specific application needs primarily defined by the rock being drilled. Relying on physical rock scraping tests is no longer sustainable considering the formation variety and ever-growing development cost.

In this paper, we propose a new methodology to iterate 3DC shape design more efficiently and accurately through virtual cutter rock interaction (CRI) enabled by digital rock lab (DRL) –a physics-based virtual CRI testing platform where a library of virtual rocks is digitalized to represent different formations including carbonate, sandstone, and shale, etc. Virtual rock scraping tests are conducted to evaluate the cutting efficiency and cutter durability for a specific cutter shape and formation rock pair. Moreover, the output reaction forces can be exported into the SLB proprietary drilling software IDEAS * integrated dynamic design and analysis platform for bit drilling dynamics simulation. A case study is also given on how an application-specific hyperbolic diamond cut element (HDE) is developed through DRL for this specific Haynesville Shale lateral drilling in the southern USA. We have completed 34 plus field tests to date with an average 53.5% rate of penetration improvement.

Introduction

In recent years, there has been a rapid growth of three-dimensional cutter (3DC) usage in drill bit applications all over the world. The 3DCs usually refer PDC cutters that are manufactured with a nonplanar diamond top work surface. **Fig. 1** shows a family of unique 3DC shapes that were developed for various formation drilling needs over the last 10 years.

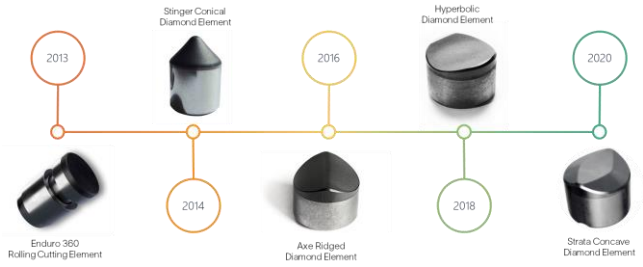

Fig. 1–Brief timeline of SLB three-dimensional cutter offerings.

With today's synthetic diamond technology, laser machining can quickly build a 3DC shape out of almost any diamond grade selection within a matter of weeks, even days. Design features can be micromachined precisely and efficiently with an ultrafast femtosecond laser (Ali, Litvinyuk, and Rybachuk, 2021). However, challenges remain when it comes to the design and development of an application-specific 3DC cutter shape. Understanding the CRI between any new 3DC and the target application is important.

Historically, development of an application-specific 3DC relies heavily on physical lab testing. As shown in **Fig. 2,** the development usually starts with understanding the target formation characteristics. Then, the 3DC shape is iteratively optimized for the highest cutting efficiency in this application. In this regard, a typical rock scraping test is conducted to understand the cutter rock interaction (CRI) between different 3DC shape iterations and the target rock. Rock is usually submerged in a pressurized environment to simulate its strength at the target drilling depth. In addition, diamond durability is also verified in lab verification and validation (V&V) tests to make sure the 3DC shape can last through the run. The CRI reaction forces are collected from the physical rock scraping tests and can be input into a proprietary drilling dynamics simulation platform (i.e. IDEAS platform) for bit cutting structure design (Huang and Cariveau 2010). Afterward, the new 3DC will be deployed into field testing for the final validation.

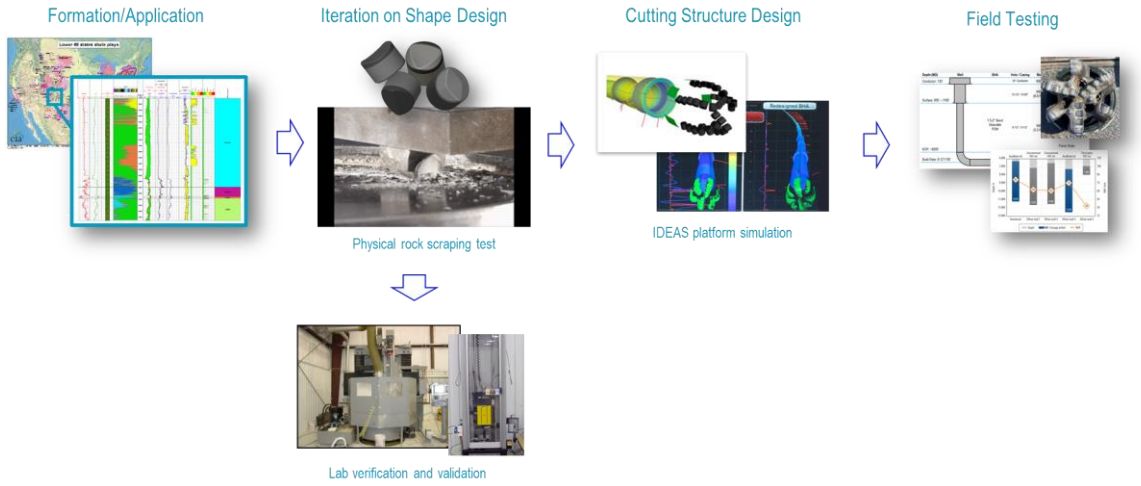

Fig. 2–Physical testing based 3DC development flowchart.

Over the years, more than 24 thousand sets of physical rock scraping test data are collected for PDC cutters and tested in various types of rocks and under different confining pressures (Panayirci, Skoff, and Shen, 2022). Similar physical experiments are also performed by both service companies and academic institutes to study the mechanical specific energy (MSE) of PDC cutter rock cutting under confining pressures (Rafatian, et al., 2010, Zhou, et al., 2012).

The physical-testing-based methodology has been adopted over the last 15 years for 3DC shape development. Following this method, multiple 3DC shapes are developed to improve drilling efficiency in various applications. For example, a ridged diamond element (RDE) was developed to improve rate of penetration (ROP) in the Granite Wash Formation and saved customers 24% in cost (Crane, et al., 2017); a HDE is delivered to improve curve and lateral drilling ROP in the Denver-Julesburg (DJ) Basin by 13% (Santana, et al., 2019).

However, the lab testing heavy methodology is becoming less and less sustainable due to the increasing demand for application-specific 3DC solutions. The laborious rock scraping test is both challenging and time consuming. Therefore, we urgently need a new methodology for 3DC development and delivery so the customer's application-specific needs can be met quickly.

New 3DC Development Methodology By Digital Rock Lab (DRL)

A new methodology is developed to accelerate the 3DC shape design and development iteration by minimizing the need to conduct physical testing as shown in **Fig. 3.** The physical rock scraping test as shown in Fig. 2 is replaced by a series of high-fidelity CRI simulations. The DRL is a physics-based virtual cutter rock interaction modeling and simulation platform where new 3DC shapes can be evaluated for rock cutting efficiency. In addition, with a library of digitalized rock models, the 3DC shape can be quickly tested through a virtual rock cutting process and iterate to achieve a fast application-specific cutter shape solution. A virtual V&V strategy is also enabled by simulating loading from a realistic downhole cutter rock interaction.

The foundation of building the DRL is to establish a rock formation library that can provide rock parameters to simulate different formations under different confined pressure or depth. In this regard, we conduct a series of typical core sample tests, i.e., triaxial compression (TC) tests as shown in **Fig. 4,** to convert a physical rock sample into a digitalized format and utilize it to simulate the rock's pressure-dependent failure mechanism in a virtual CRI process.

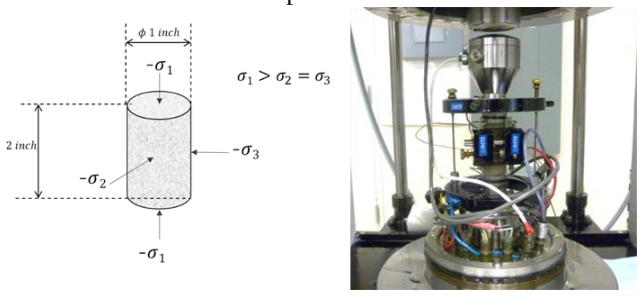

Fig. 3–Principal stress state and core sample size (left) in a typical triaxial compression test (right).

To be more specific, we measure the critical Mohr-Coulomb (M-C) plasticity model parameters in such TC tests. Then, the M-C model parameters are converted into those of a more computational-friendly Drucker-Prager (D-P) model. For example, parameters of a linear D-P model can be obtained by matching the parameters in a linear M-C model (Jiang and Xie, 2011) (See Appendix A).

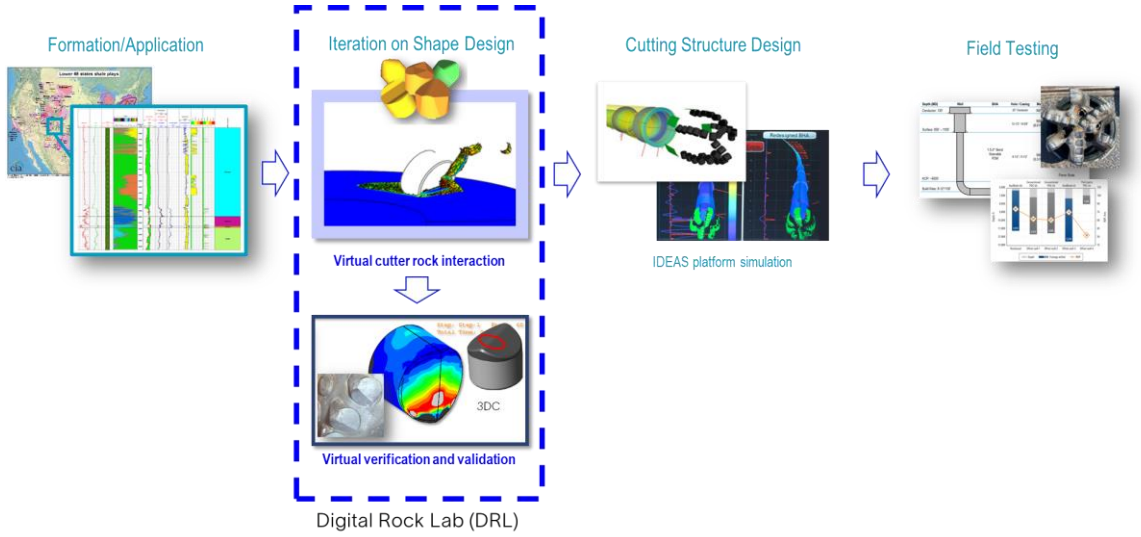

Fig. 3–Proposed virtual testing based 3DC development flowchart.

The available digital rocks that are tested from TC tests are shown in **Table 1.** In total, 10 different types of rocks are available in DRL, which includes 1 carbonate, 3 limestones, 4 sandstones, 1 carbonate, 1 evaporate, and 1 shale. We have selected, tested, and digitalized these benchmark rocks to ensure a coverage of formations with different strengths. For example, from a very soft shale (<5,000 psi) to an extreme hard limestone (> 40,000 psi). Each type of rock has been tested under at least four different confining pressures (for example, 100 psi, 1,500 psi, 3,000 psi, and 9,000 psi) to obtain its M-C parameters. The rock parameters are further calibrated and verified with the legacy lab testing data (Panayirci, Skoff, and Shen, 2022) before they are released for virtual CRI simulation in DRL.

For DRL, we have chosen the D-P model with ductile damage initiation and propagation rule as the rock constitutive law for its robustness in terms of simulating rock removal. The commercial explicit Finite Element Analysis (FEA) solver (i.e., ABAQUS Explicit) is used for its relatively low computational cost and higher efficiency when compared with the implicit FEA solver.

Table 1–Digitalized Rock Library

Digitalized Rock Type	Unconfined compressive strength (USC) (10^3 psi)	M-C slope angle (deg)
Limestone A	5–10	17
Limestone B	20–25	28
Limestone C	40–45	25
Sandstone A	10–15	25
Sandstone B	15–20	32
Sandstone C	20–25	40
Sandstone D	25–30	45
Carbonate	20–25	29
Evaporate	2–5	15
Shale	2–5	10

Case Study: 13 mm 3DC Development for Haynesville Curve and Lateral Application

In early 2022, an opportunity came up in the 6.75-in curve and lateral drilling application in the Arkansas–Texas Basin of US Land. Operators are looking for cutter solutions to improve their performance in this Haynesville shale application. The target formation is mainly Bossier Shale and Haynesville Shale with a total vertical depth (TVD) at around 10,500 ft **(Fig. 5).** Usually, in the curve and lateral drilling, a 5-6/7 in 8 stage 0.79 RPG 2.25° bend motor is used and 8–10 deg/100 ft build rate is desired. The bend motor angle will be set at 1.8° for the lateral section. Overall, the application itself is very benign and usually only cold PDC cutters are needed. To further improve performance and specifically increase ROP, the operators are in immediate need for a 13 mm 3DC cutter solution for this specific drilling application.

Based on the operator needs and application requirement, we have set our strategy to utilize DRL to provide a fast 3DC design solution. The HDE shape has been selected for the development due to its high efficiency in soft formation drilling (Santana, et al., 2019). The digitalized shale (UCS 2,000–5,000 psi) is also selected to represent the Haynesville Formation in the virtual CRI experiments. In addition, the digitalized carbonate (UCS 20,000–25,000 psi) is also added to simulate a hard stringer in virtual frontal impact experiments.

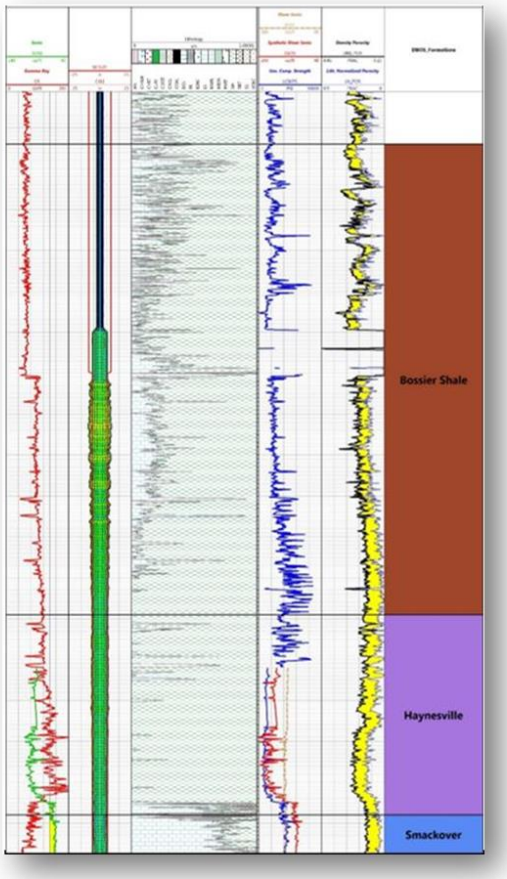

Fig. 5–Haynesville Basin formation properties and typical geological locations.

Design of Virtual Experiment 1: Shape Impact Resistance

The key feature of an HDE shape is its positive rake effect. This is achieved by a key offset angle dimension α on the diamond top surface as shown in **Fig. 6.** The effective CRI angle γ between a HDE and rock interaction is equal to β-α and HDE is working at positive rake when $\gamma < 0$. Inappropriate offset angle design is either unnecessary as the cutter back rake (BR) is limited by the cutting structure, or harmful since an overly aggressive offset angle can cause premature cutter impact failure. Based on the baseline 6.75 in-Y513 bit design, we focus on two different 13 mm HDE iterations that are distinguished by offset angle as shown in the same figure. HDE-A is slightly more aggressive design with an offset angle of 20˚ and HDE-B is less aggressive with offset angle set at 15˚.

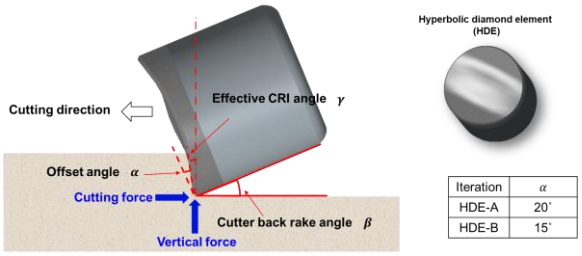

Iteration	α
HDE-A	20˚
HDE-B	15˚

Fig. 6–Illustration and dimension definition for HDE.

As shown in **Fig. 7,** in the virtual frontal impact experiment, the HDE is setup with the assumption that it is suddenly impacted by the formation when it is located on the shoulder of a drill bit. The impact DOC is 0.080 in. The impact velocity v is obtained by assuming that HDE is at a 3-in bit radius and the bit rotation is 300 rpm. As a comparison, the flat PDC cutter is also included as a baseline.

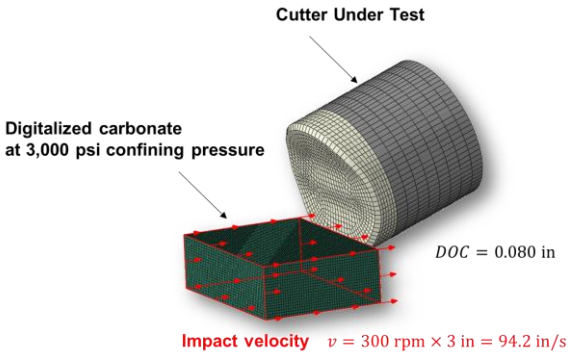

Fig. 7–Virtual frontal impact experiment setup (use HDE as example).

The results are shown in **Fig. 8** as the maximum level of max principal stress on the cutter top surface during a CRI impact is obtained. It is found that under the same impact energy, the HDE-A iteration shows slightly lower frontal impact resistance than flat PDC cutter with 3% higher stress level. While HDE-B has shown an improved frontal impact resistance than flat PDC cutter with 10% stress reduction during the same impact. By adding a 5˚ side rake angle, the frontal impact resistance of HDE-B can be further improved by reducing max stress level by 15% in total when compared with the flat PDC cutter.

As a result, the HDE-B design with a 15˚ offset angle has been selected to move forward and it will be referred to as hyper 3DC for the following sections.

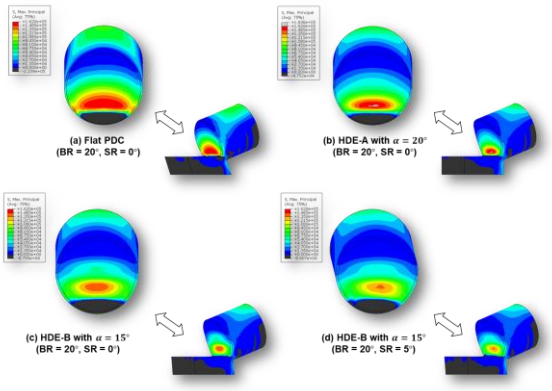

Fig. 8–Highest max principal stress contour recorded from virtual frontal impact experiment.

Design of Virtual Experiment 2: Shape cutting efficiency

The next virtual experiment conducted is to evaluate the new hyper 3DC cutting efficiency in the target Haynesville application. In this study, the digitalized shale (2,000 – 5,000 psi UCS) at 3,000 psi confining pressure is selected to represent the Haynesville Shale for cutting efficiency evaluation. The virtual CRI setup is shown in **Fig. 9.**

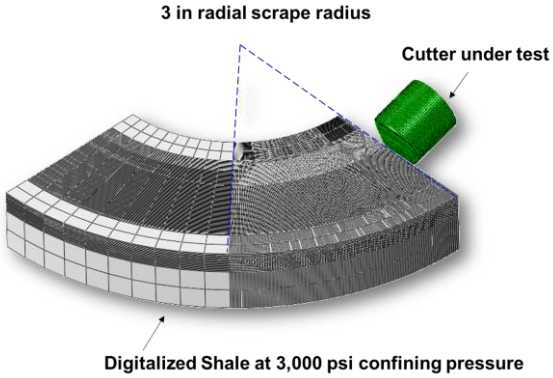

Fig. 9–Virtual CRI setup for cutting efficiency (Use hyper 3DC as an example).

The test matrix at different depth of cut (DOC)s, BR angles and side rake (SR) angles are shown in Table 2. The BR angle of interest is 15˚ to 20˚ and the SR angle of interest is 0˚ to 5˚. The range is decided based on the baseline bit design for field testing. The CRI experiments are conducted from very low DOC of 0.020 in, to a medium to high DOCs of 0.080 in and 0.160 in. The extreme 0.250 in DOC is also included in experiments. Again, a flat PDC cutter is also included for cutting efficiency comparison.

Table 2–Virtual CRI Simulation Design of Experiments

Back Rake Angle (˚)	DOC (in)	Side Rake Angle (˚)
10	0.020, 0.080, 0.160, 0.250	0,5
15	0.020, 0.080, 0.160, 0.250	0,5
20	0.020, 0.080, 0.160, 0.250	0,5

From each virtual CRI experiment, the time sequence of vertical force and cutting force between cutter rock interface can be recorded (See **Fig.B.2-B.5**). The time sequence of vertical force and cutting force are further processed by reading the 90 percentile force values plotted against the depth of cut. The comparison between hyper 3DC and flat PDC at different BR angles are shown in **Fig. 10**, **Fig. 11** and **Fig. 12**.

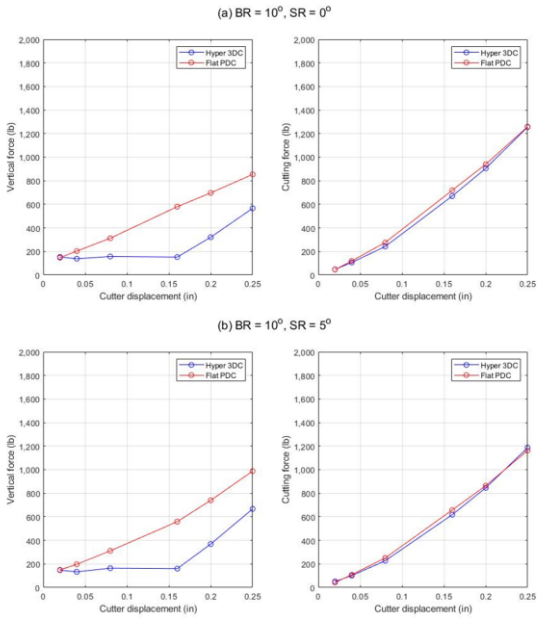

Fig. 10–Vertical force and cutting force at 90 percentile versus depth of cut (hyper 3DC against flat PDC at BR 10˚).

Fig. 10 shows that at 10˚ BR angle, the hyper 3DC is the most efficient with minimum vertical force increase with depth of cut up to 0.160 in. And the maximum vertical force difference seen between hyper 3DC and flat PDC is around 73% at 0.160 in depth of cut. The cutting force of hyper 3DC is similar and slightly lower than flat PDC at 10˚ BR angle. This is due to a higher cutting efficiency in soft shale with a positive rake angle.

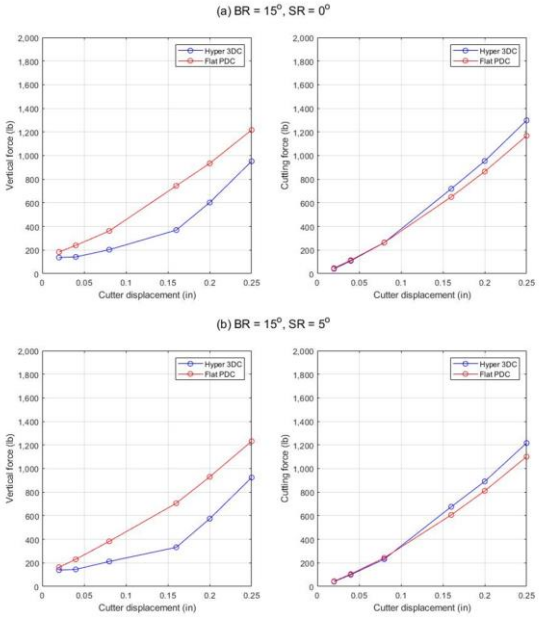

Fig. 11–Vertical force and cutting force at 90 percentile versus depth of cut (hyper 3DC against flat PDC at BR 15˚).

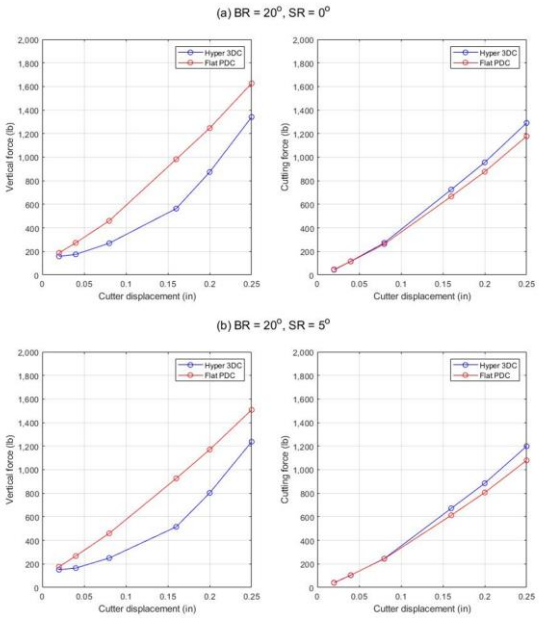

Fig. 12–Vertical force and cutting force at 90 percentile versus depth of cut (hyper 3DC against flat PDC at BR 20˚).

From **Fig. 11** and **Fig. 12,** it is shown that hyper 3DC still shows a significant vertical force reduction at 15˚ and 20˚ BR angle with about 39%–51% difference at 0.160 in depth of cut. However, the aggressiveness of hyper 3DC is increasing and cutting force starts to be higher than flat PDC cutter after 0.080-in depth of cut. It is likely due to the effective CRI angle γ of hyper 3DC gradually transition into negative rake angle range when the cutter BR angle is larger than 15˚. In addition, the virtual CRI experiment results are visualized in **Fig. 13** and **Fig. 14** to show the rock cutting morphology difference between the flat PDC cutter and hyper 3DC.

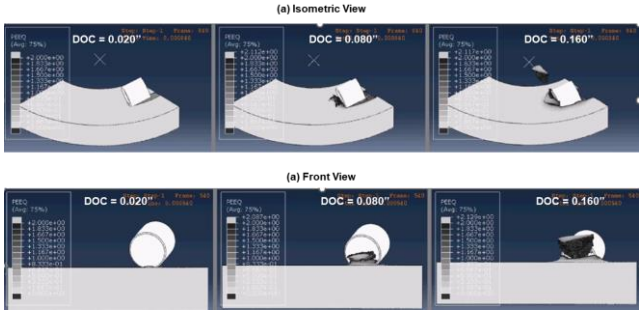

Fig. 13–Cutting morphology visualization from virtual CRI experiment in digitalized shale (flat PDC).

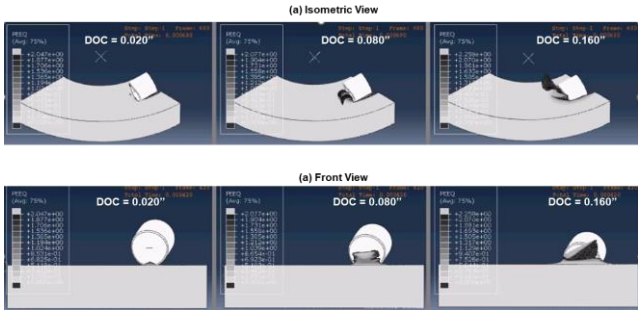

Fig. 14–Cutting morphology visualization from virtual CRI experiment in digitalized shale (hyper 3DC).

Design of Experiment 3–Bit Drilling Dynamics

The vertical force and cutting force are further imported to the IDEAS platform for a bit level dynamic simulation to evaluate the bit performance improvement with the proposed 13 mm hyper 3DC drop-in. The hyper 3DC is dropped onto the shoulder area of a baseline Smith Bits 6.75 in SDi513 bit design where the cutter BR angles ranges from 10˚ to 18.75˚ with majority of the cutter BR angles are at 10˚. This is the desired BR range to maximize hyper 3DC's cutting efficiency in shale. Meanwhile, the bit design also incorporates 5˚ SR angle for all the drop-in hyper 3DCs for better durability. The cutting structure layout is shown in **Fig. 15.** For simulation, typical Haynesville lateral drilling parameters are assumed with total rpm set at 300 and WOB varies from 10 klb to 40 klb.

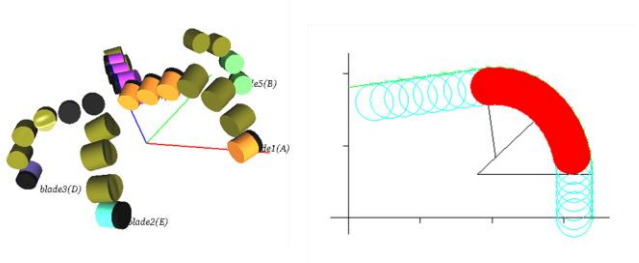

Fig. 15–Testing Smith Bit 6.75-in Y513S design (SDi513 with 13 mm hyper 3DC on shoulder)

The simulation results are shown in **Fig. 16.** From the simulated WOB and rpm combination, the hyper 3DC dropped-in bit is expected to improve ROP by 30.3% to 35.9%. This has confirmed the 3DC design from systematic level and verified bit performance before field testing.

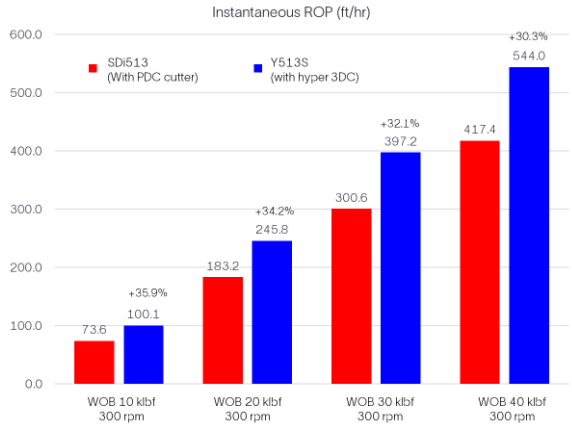

Fig. 16–Bit dynamics results using virtual CRI forces.

Hyper 3DC Field Performance

Upon completing all the virtual CRI experiments, the optimized hyper 3DC shape is quickly laser machined onto a baseline 13 mm PDC cutter grade of selection as shown in **Fig. 17.** The laser etched hyper 3DCs are dropped into the Smith Bits 6.75-in SDi 513 design to form the new 6.75-in Y513S bits for field testing since June 2021.

Fig. 17–A 13 mm laser etched application-specific hyper 3DC.

To date, we have completed more than 16 Y513S field runs. A performance study is conducted to compare the baseline 6.75-in SDi513 bit and the hyper 3DC dropped-in 6.75-in Y513S bit with field run data recorded in the DRS* drilling record system by SLB from July 2022 to January 2023.

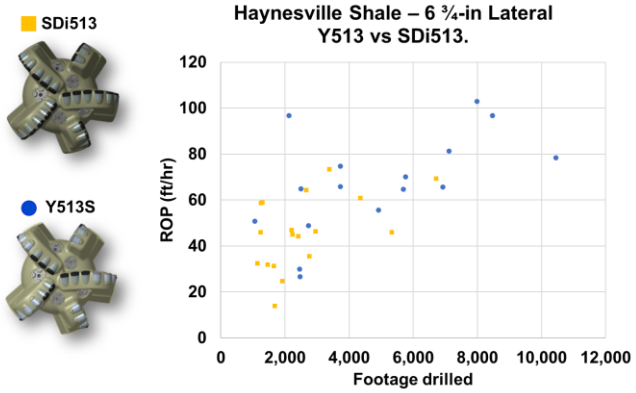

Fig. 18–Field performance comparison between 6.75-in SDi513 and Y513S.

The data points shown in **Fig. 18** only consider runs within Haynesville lateral and run footage is more than 1,000 ft. Total 22 rigs are found with 34 valid runs, including 18 runs of 6.75-in SDi513 bits and 16 runs of 6.75-in Y513S bits. Based on the existing results, the average ROP for the baseline SDi513 runs is 43.73 ft/hr and the average ROP for the hyper Y513S runs is 67.12 ft/hr. It is shown that with properly placing the 13 mm hyper 3DC on the baseline bit, the Y513S bit can deliver an average of 53.5% increase in rate of penetration (ROP) when compared with the baseline SDi513 bit from the current run results. The current ROP improvement met and exceeded what we expected from the virtual development.

As for bit dull condition, the 13 mm hyper 3DC has shown similar dull grading as the baseline PDC cutter with most of the runs coming out green. As an example, a Y513S bit run (s/n JV8295) in Haynesville lateral is shown in **Fig. 19.** The bit drilled 8,467 ft to TD from 12,877 ft depth-in to 21,344 ft depth-out and achieved a IADC ROP of 96.77 ft/hr. The bits come out with a dull grading of 1–2 worn teeth on shoulder as shown in **Fig. 20.** As expected, the hyper 3DC showed very comparable dull condition as the baseline flat PDC cutter. However, a more wear-resistant base PDC cutter grade could be selected to address the wear dull and further improve the bit performance.

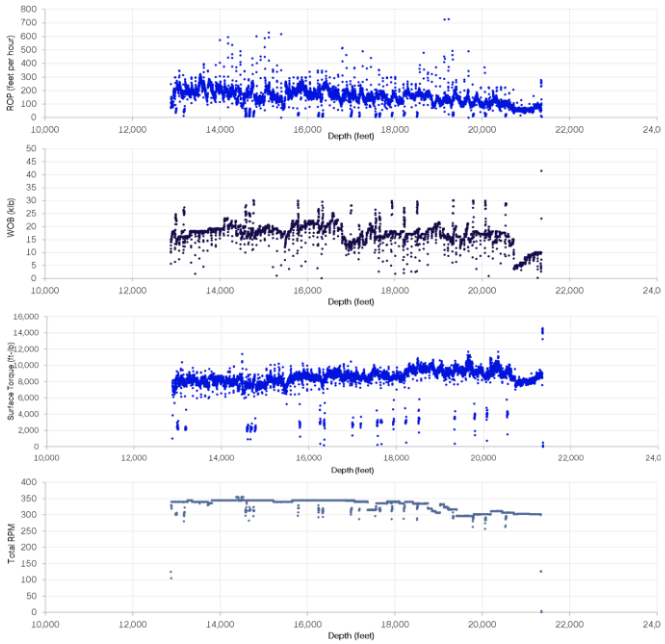

Fig. 19–JV8295 6.75-in Y513S field run data.

Performance Details	
DEPTH IN	12,877 ft
DEPTH OUT	21,344 ft
DRILLED FEET	8,467 ft
IADC HOURS	87.5 hrs
IADC ROP	96.77 ft/hr
DULL GRADING	1-2-WT-S-XXX-IN-BT-TD

Fig. 20–JV8295 6.75-in Y513S cutter dull pictures after run.

Conclusions

A new 3DC development methodology is introduced that minimizes the need for laborious physical testing and accelerates the application-specific cutter shape iteration. The DRL platform enables a virtual verification and validation strategy that is based on high-fidelity CRI simulations. The physics-based simulation is enabled by advanced finite element modeling and a library of digitalized rock samples. In DRL, a cutter shape can be quickly evaluated for its durability and cutting efficiency in the target rock formation. The output from DRL can be directly input into the IDEAS platform for bit level drilling dynamics evaluation.

The proposed methodology is adopted in the rapid development of a 13 mm hyper 3DC for the 6.75-in curve and lateral section in the Haynesville Basin. The new HDE shape is iteratively designed and verified in DRL and is dropped into a SDi513 bit for field testing. To date, we have completed 16 field test runs. Results show that the application-specific hyper 3DC has improved ROP by an average 53.5% with similar durability as the baseline PDC cutter.

Following the new methodology, the new hyper 3DC has met and exceeded our expectations and has proved the effectiveness and efficiency of the new DRL based methodology. We plan to adopt DRL as the virtual V&V strategy for application-specific 3DC shape development in the future. However, the current DRL prediction is more on the conservative side, which means that we still need to improve our digital rock representation from a more realistic downhole condition. In this regard, more focus will be put onto rock digitalization methodology based on real formation characteristics through a data-driven approach.

Acknowledgments

The authors wish to express their gratitude to SLB for permission to release the simulation results and field performance data. Thanks to the DBOS* drill bit optimization system team of SLB for providing the application lithology graph.

Nomenclature

DBOS = *Drill bit optimization system of SLB*
DRS = *Drilling record system of SLB*
IDEAS = *Integrated dynamic design and analysis platform of SLB*
RPG = *Revolution per gallon*
V&V = *Verification and validation*

*Mark of SLB

References

Ali, B., Litvinyuk, I.V. and Rybachuk, M., 2021. "Femtosecond Laser Micromachining of Diamond: Current Research Status, Applications and Challenges," *Carbon*, 179, July, pp 209–226 https://doi.org/10.1016/j.carbon.2021.04.025

Crane, D., Zhang, Y., and Douglas, C., et al., 2017. "Innovative PDC Cutter with Elongated Ridge Combines Shear and Crush Action to Improve PDC Bit Performance," Paper presented at the SPE Middle East Oil & Gas Show and Conference, Manama, Kingdom of Bahrain, March SPE-183984-MS https://doi.org/10.2118/183984-MS

Huang, S.J. and Cariveau, P.T., Smith International Inc, 2010. "Methods for Modeling, Displaying, Designing, and Optimizing Fixed Cutter Bits," U.S. Patent 7,693,695

Jiang, H. and Xie, Y., 2011. "A Note on the Mohr–Coulomb and Drucker–Prager Strength Criteria," *Mechanics Research Communications*, Vol 38, Issue 4, pp 309–314 https://doi.org/10.1016/j.mechrescom.2011.04.001

Panayirci, H.M., Skoff, G., and Shen, Y., 2022, "Design and Analysis of a Comprehensive Database Containing 24,000 Polycrystalline Diamond Compact Cutter Scrape Tests," Paper presented at the IADC/SPE International Drilling Conference and Exhibition, Galveston, Texas, USA, March SPE-208674-MS https://doi.org/10.2118/208674-MS

Rafatian, N., Miska, S., and Ledgerwood, L.W., et al., 2010. "Experimental Study of MSE of a Single PDC Cutter Interacting with Rock Under Simulated Pressurized Conditions," *SPE Drilling & Compl*, Vol 25, Issue 01, pp 10–18 SPE-119302-PA https://doi.org/10.2118/119302-PA

Santana, R., Skoff, G., and Krough, B., et al., 2019, "Development, Testing, and Deployment of a New Hyperbolic Diamond Element Bit in DJ Basin of Colorado," Paper presented at the Abu Dhabi International Petroleum Exhibition & Conference, Abu Dhabi, UAE, November SPE-197416-MS https://doi.org/10.2118/197416-MS

Zhou, Y., Zhang, W., and Gamwo, I.K., 2012, "Mechanical Specific Energy vs. Depth of Cut," Paper presented at the 46th US Rock Mechanics/Geomechanics Symposium, Chicago, Illinois, June ARMA-2012-622

Appendix–A: Converting Linear Mohr-Coulomb (M-C) Model to Linear Drucker-Prager (D-P) Model

Eq. 1 is a linear M-C model where τ is the maximum shear stress (half of the maximum and minimum principal stress), c is the material cohesion, and ϕ is the slope angle of linear M-C yield surface.

$$\tau = c - \sigma \tan \phi \quad (1)$$

Eq. 2 is a linear D-P model where t is the Von Mises stress, p is the mean stress, β is the slope angle of the linear D-P yield surface and d is the cohesion of material.

$$t = p \tan \beta + d \quad (2)$$

The relationship between the frictional angle and cohesions are shown in **Eq. 3** and **Eq. 4.**

$$\tan \beta = (6 \sin \phi)/(3 - \sin \phi) \quad (3)$$

$$d = (6c \cos \phi)/(3 - \sin \phi) \quad (4)$$

Appendix – B: Time sequence of vertical force and cutting force from Design of Virtual Experiment 2 (Shape cutting efficiency)

The time sequence of reaction force data that are used to generate Figures 10-12 is shown in Figure B.1 to Figure B.6.

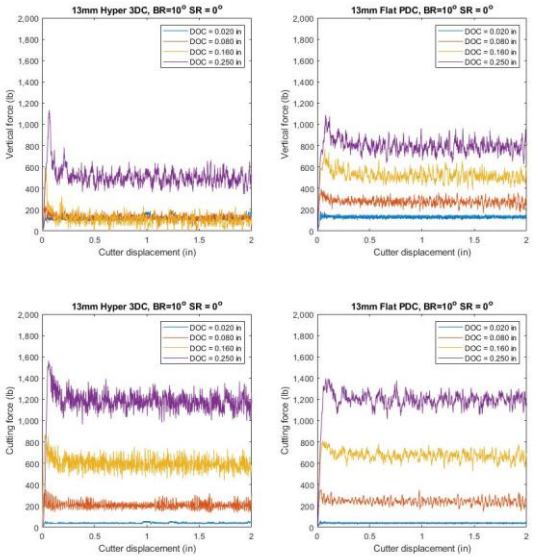

Figure B.1 – Vertical force and cutting force from Virtual CRI (BR = 10˚, SR = 0˚): Hyper 3DC (left) and Flat PDC (right)

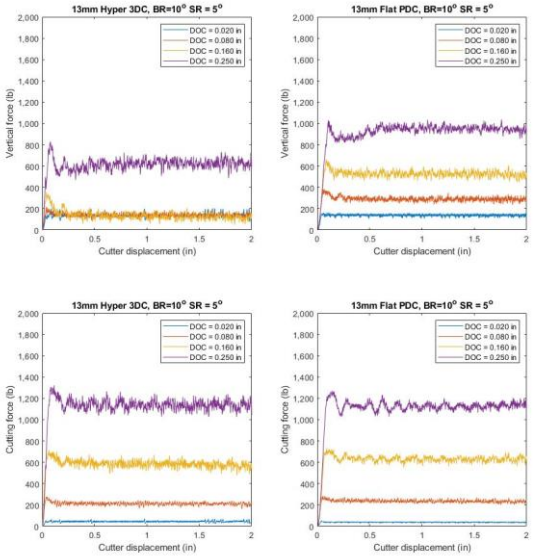

Figure B.2– Vertical force and cutting force from Virtual CRI (BR = 10˚, SR = 5˚): Hyper 3DC (left) and Flat PDC (right)

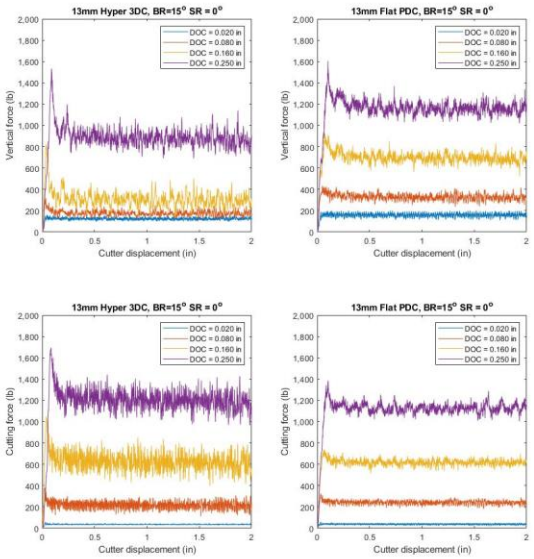

Figure B.3– Vertical force and cutting force from Virtual CRI (BR = 15˚, SR = 0˚): Hyper 3DC (left) and Flat PDC (right)

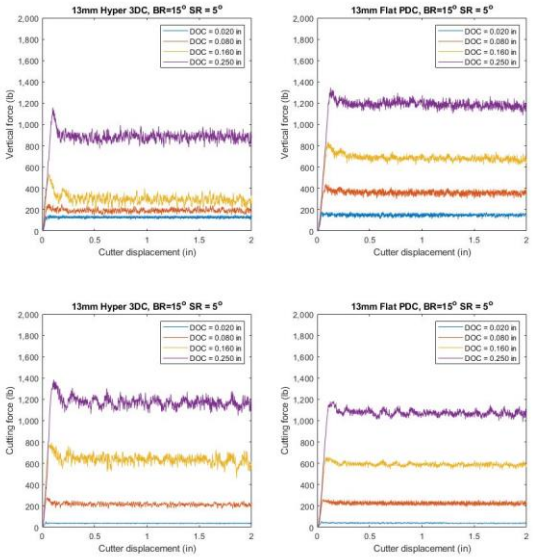

Figure B.4– Vertical force and cutting force from Virtual CRI (BR = 15˚, SR = 5˚): Hyper 3DC (left) and Flat PDC (right)

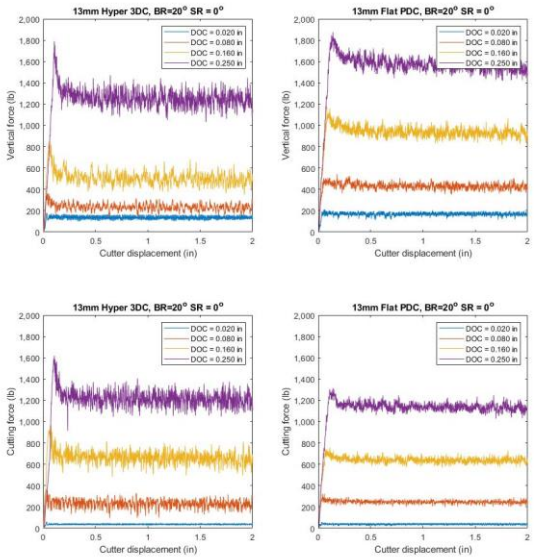

Figure B.5– Vertical force and cutting force from Virtual CRI (BR = 20˚, SR = 0˚): Hyper 3DC (left) and Flat PDC (right)

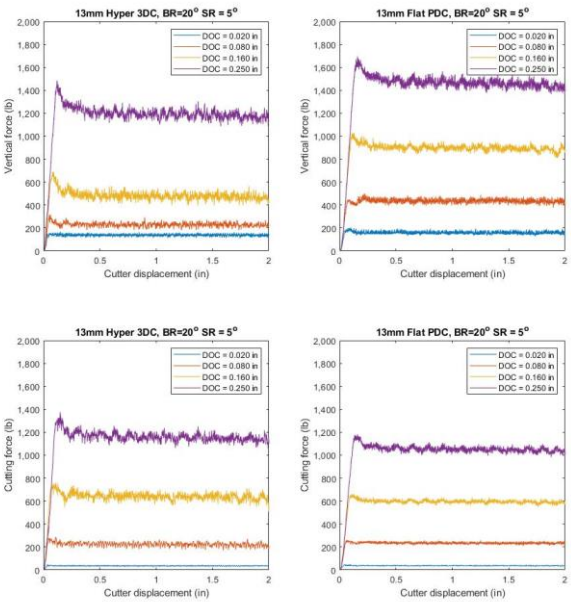

Figure B.6– Vertical force and cutting force from Virtual CRI (BR = 20˚, SR = 5˚): Hyper 3DC (left) and Flat PDC (right)